

Real-Time Orbit Feedback at the APS

J.A. Carwardine and F.R. Lenkszus

*Advanced Photon Source, Argonne National Laboratory, 9700 South Cass Avenue,
Argonne, IL 60439, USA*

A real-time orbit feedback system has been implemented at the Advanced Photon Source in order to meet the stringent orbit stability requirements. The system reduces global orbit motion below 30Hz by a factor of four to below 5 μ m rms horizontally and 2 μ m rms vertically. This paper focuses on dynamic orbit stability and describes the all-digital orbit feedback system that has been implemented at the APS. Implementation of the global orbit feedback system is described and its latest performance is presented. Ultimately, the system will provide local feedback at each x-ray source point using installed photon BPMs to measure x-ray beam position and angle directly. Technical challenges associated with local feedback and with dynamics of the associated corrector magnets are described. The unique diagnostic capabilities provided by the APS system are discussed with reference to their use in identifying sources of the underlying orbit motion.

RECEIVED
SEP 21 1999
OSTI

INTRODUCTION

The Advanced Photon Source (APS) is the foremost third-generation synchrotron light source in the United States, delivering intense x-rays to as many as 35 insertion-device and 35 bending-magnet beamlines. Orbit stability of the stored particle beam is critical to achieving optimum performance for the x-ray users. At the APS, the rms orbit motion is not to exceed 5% of the particle beam size, and with the design 10% x-y coupling, this translates to horizontal and vertical stability requirements of 17 μ m rms and 4.5 μ m rms, respectively.

This level of stability requires active feedback to reduce orbit motion from sources such as vibration (e.g., from ground motion) and from magnet power supply fluctuations that modulate the magnetic fields guiding the particle beam around the storage ring.

The APS orbit feedback system is designed to provide dynamic correction of low frequency orbit disturbances, both on a global rms basis (long spatial wavelengths) and locally at each x-ray source point (local feedback). The global orbit feedback system has been in routine operation with the APS users since June 1997 and corrects orbit motion up to approximately 50Hz.

The submitted manuscript has been created by the University of Chicago as Operator of Argonne National Laboratory ("Argonne") under Contract No. W-31-109-ENG-38 with the U.S. Department of Energy. The U.S. Government retains for itself, and others acting on its behalf, a paid-up, nonexclusive, irrevocable worldwide license in said article to reproduce, prepare derivative works, distribute copies to the public, and perform publicly and display publicly, by or on behalf of the Government.

DISCLAIMER

This report was prepared as an account of work sponsored by an agency of the United States Government. Neither the United States Government nor any agency thereof, nor any of their employees, make any warranty, express or implied, or assumes any legal liability or responsibility for the accuracy, completeness, or usefulness of any information, apparatus, product, or process disclosed, or represents that its use would not infringe privately owned rights. Reference herein to any specific commercial product, process, or service by trade name, trademark, manufacturer, or otherwise does not necessarily constitute or imply its endorsement, recommendation, or favoring by the United States Government or any agency thereof. The views and opinions of authors expressed herein do not necessarily state or reflect those of the United States Government or any agency thereof.

DISCLAIMER

**Portions of this document may be illegible
in electronic image products. Images are
produced from the best available original
document.**

ORBIT CORRECTION PRINCIPLES

The principles of orbit correction have been covered extensively in the literature [1]. A linear response matrix describes the relationship between small changes in chosen corrector magnet (dipole) fields and the resulting change in the particle beam orbit as measured at chosen beam position monitors (BPMs). This is described mathematically by the equation

$$\mathbf{R} \Delta \mathbf{c} = \Delta \mathbf{x}$$

where \mathbf{R} is the so-called response matrix, $\Delta \mathbf{c}$ is a vector of corrector field changes, and $\Delta \mathbf{x}$ is the resulting change in orbit as measured at specific BPMs. This equation can be inverted mathematically to produce a relationship that maps orbit perturbations to changes in corrector magnet fields that would cancel those perturbations. For small orbit errors, the relationship is assumed to be linear and time invariant. Different objectives, such as correcting the orbit in an rms sense or correcting specific locations, can be achieved by choice of BPM and corrector locations and by applying different weights to correctors or BPMs when computing the inverse response matrix.

At the APS, orbit correction is performed by two systems that operate independently but in parallel. A workstation-based system corrects the orbit at ten-second intervals using 80 correctors and more than 300 BPMs to compensate for slow changes in the global DC orbit and to return to a user-preferred orbit at the beginning of each fill [2]. It is also used with different selections of BPMs and correctors to make local steering changes at the x-ray source points as requested by the users.

In addition to the workstation-based system, the real-time orbit feedback system that is the subject of this paper performs orbit corrections at a 1kHz rate. It uses 160 BPMs and 38 correctors to correct dynamic orbit errors and incorporates a high-pass filter to roll off the response below 20mHz. Orbit corrections below this frequency are performed by the workstation-based system.

Implementation of the Global Algorithm

Inspection of the orbit correction algorithm reveals that the calculation of each new corrector setpoint requires forming the vector dot product of the appropriate row of the inverse response matrix and the entire vector of measured BPM values (or 'errors' from the desired values). Since there are 38 correctors used in each plane, a total of 38 vector dot products must be computed to complete one correction step.

In the APS system, the computations are distributed between 20 VME crates (described in the next section), with each crate computing only the dot products associated with its correctors, as shown in Figure 1. The results of each vector dot product become the input to a control loop around each corrector.

$$\begin{array}{c}
 \text{inverse response matrix} \\
 \left(\begin{array}{c}
 \text{Crate 1/2} \\
 \left\{ \begin{array}{c} \text{row 1} \\ \text{row 2} \end{array} \right. \end{array} \right. \\
 \left. \begin{array}{c} \text{Crate 3/4} \\
 \left\{ \begin{array}{c} \text{row 3} \\ \text{row 4} \end{array} \right. \end{array} \right. \\
 \left. \begin{array}{c} \text{Crate 39/40} \\
 \left\{ \begin{array}{c} \text{row 39} \\ \text{row 40} \end{array} \right. \end{array} \right. \\
 \cdot \left[\begin{array}{c} \text{BPM errors} \end{array} \right] = \left[\begin{array}{c} \text{corrector 'errors'} \\
 \left\{ \begin{array}{c} \text{corrector 1} \\ \text{corrector 2} \end{array} \right. \end{array} \right. \\
 \left. \begin{array}{c} \left\{ \begin{array}{c} \text{corrector 3} \\ \text{corrector 4} \end{array} \right. \end{array} \right. \\
 \vdots \\
 \left. \begin{array}{c} \left\{ \begin{array}{c} \text{corrector 39} \\ \text{corrector 40} \end{array} \right. \end{array} \right.
 \end{array}$$

FIGURE 1. Separation of the global algorithm across 20 slave stations.

SYSTEM IMPLEMENTATION

The APS storage ring contains a total of 360 rf BPMs and 317 dual-function corrector magnets. All of these are accessible to the APS control system (through EPICS). Additionally, 320 of the BPMs and all of the correctors can be accessed by the real-time orbit feedback system. However, unlike the workstation-based system that uses the APS control system to access BPMs and correctors, the real-time system has dedicated data links to both BPM and corrector magnet power supply hardware.

The real-time system uses a total of 20 VME 'slave' crates distributed around the circumference of the 1.1km storage ring. Each contains interfaces to 16 rf BPMs and 16 corrector magnet power supplies in each plane [3]. Every slave crate also contains digital signal processors (DSPs) that implement the real-time algorithms. The overall layout of a typical slave crate is shown in Figure 2.

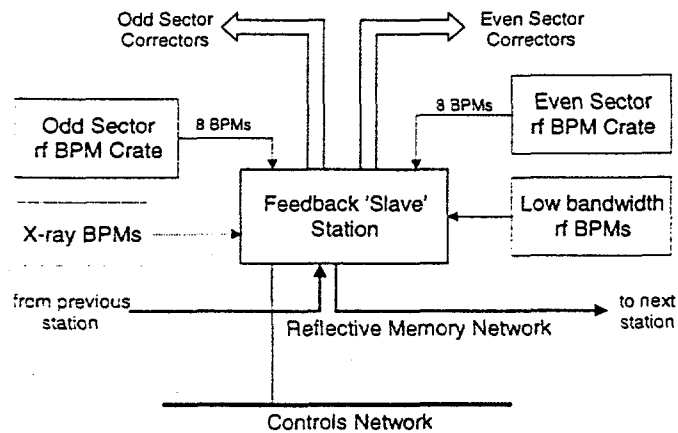


FIGURE 2. Real-time orbit feedback system layout.

A separate 'master' VME crate performs supervisory tasks and provides a central interface for data acquisition and control. All 21 VME crates communicate via a dedicated 'reflective memory' network that provides crate-to-crate data transfers at

29.6Mbytes/second. The crates are also accessible over the APS controls network. Figure 3 shows the components associated with the master and with each slave crate.

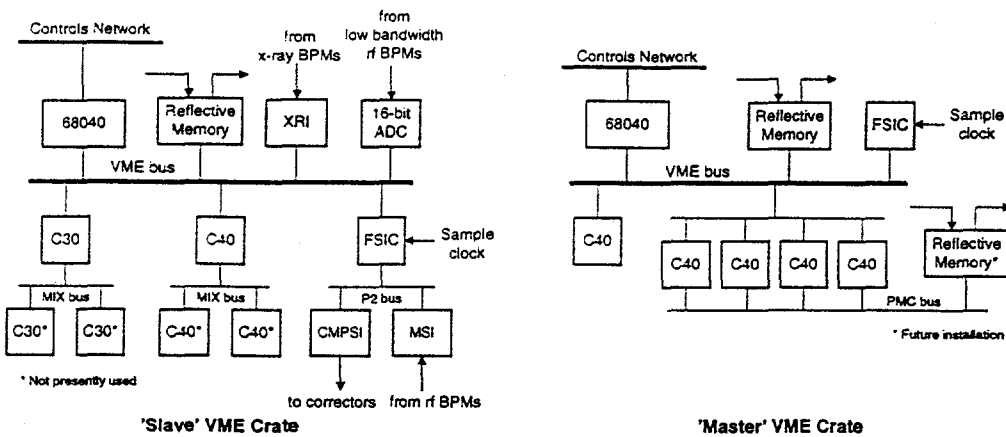


FIGURE 3. 'Master' and 'Slave' crate components.

Custom hardware receives data from the rf BPM memory scanners (MSI) and delivers setpoints to the corrector magnet power supplies (CMPSI). There are also interfaces to x-ray BPMs and to new narrow-band BPM electronics that will provide, respectively, positional feedback from the x-ray beams and more stable measurements of the particle beam position at the insertion device source points.

Both master and slave crates contain a 68040 processor that runs EPICS core routines and provides access to the DSPs via the APS controls network. Each slave crate can contain up to six DSP processors. These are commercial VME boards based on the Texas Instruments TMS320 C30 and C40 DSP processors. Presently only two of the six processors shown in the slave crate are in use, implementing global rms orbit feedback. The additional processors will be added to implement 'local' feedback at the x-ray source points.

To date, the global algorithm has been implemented with a single C40 DSP performing orbit feedback in both planes at a 1kHz rate. (The data presented here was collected with this configuration.) However, by sharing the global algorithm across two DSPs (one for each plane), we have upgraded the system to operate at 2kHz. Operation at 2kHz will be commissioned during the the APS "98-3" user run.

BPM Interface

The rf BPMs are installed at 360 locations around the storage ring, providing data every two turns. Raw BPM data flows along two separate data paths, allowing simultaneous access from the APS control system and from the real-time orbit feedback system. In order to band-limit the signal content provided to the real-time feedback system, raw BPM values are transmitted across a high-speed serial link to a 32-point boxcar averager in the orbit feedback slave crate. The averager was originally designed for orbit feedback sampling rates of 4kHz, and has a -3db point around 1.85kHz. Consequently, there is an aliasing issue with the data supplied to the orbit

feedback system, the most noticeable impact of which is that synchrotron motion at 1.8kHz is aliased to 200Hz in the orbit feedback system. Fortunately this does not lie within the correction bandwidth of the system, but does influence certain measurements using the orbit feedback data path.

A new BPM filtering module is under development that will implement multi-stage decimation filters on an embedded DSP chip right at the data source. Filtered data will be available at several bandwidths and sampling rates consistent with their uses by the orbit feedback system and by the APS control system. The new module will also resolve some data integrity and reliability problems with the high-speed serial link that transfers the raw data values at 135kHz to the orbit feedback system averager.

Corrector Interface

Each corrector power supply can receive setpoints from one of two sources, either from the APS control system as an EPICS process variable, or over a serial link from its associated orbit feedback slave crate. An electronic switch (controlled through EPICS) selects the source of the setpoints.

By throwing the switch to the EPICS source, the real-time feedback system can be completely isolated from the accelerator. This has proven very useful during commissioning and system debugging. An equally important feature is that the setpoint source can be changed 'on the fly' when beam is being delivered to the users. To do this, it has been necessary to guarantee that there are no transients on the output of the power supplies when the source is changed. When the orbit-feedback control loops are opened, the original DC setpoint (read from EPICS) is automatically copied to the power supply by the orbit feedback system through its dedicated link. With the control loops closed, the DC setpoint is used as a bias that is added to the setpoint calculated in real time by the DSPs.

Originally setpoints were transmitted by the orbit feedback system hardware only once at the end of each feedback cycle (every 1ms). However, it was found that transmission errors could cause a sufficiently large transient on the output of the power supply such that stored beam would be dumped. In addition to having improved transmission reliability, setpoints are now sent out repeatedly, at 64 μ s intervals, regardless of whether a new setpoint has been calculated. While this in itself does not prevent the errors, it does limit the duration of the transient so that the effect on stored beam is minimal.

Data Sharing and Synchronization

The processes on the 21 feedback crates (master plus 20 slaves) must be synchronized for the system to operate properly. A feedback clock (currently 1 kHz, but soon to be 2 kHz), is generated by the APS timing system processor in the main control room and distributed via the APS timing event system [4] to each of the 21 locations. Each feedback crate receives these timing tics in a custom module containing a counter and a missing pulse detector. Each DSP waits for the counter to increment from zero, at which time it begins its algorithm. A counter value greater

than 1 indicates the DSP is late. The missing pulse detector indicates a timing tic was late or missing. Both conditions are checked by the DSP and, if they occur, are reported to the control system.

Each DSP collects its local BPM data, computes BPM error values, and deposits them at the appropriate location in the BPM error vector in reflective memory. Each DSP needs the entire vector to compute its corrector values. This operation is synchronized via the reflective memory. After writing BPM error values to reflective memory, each DSP writes a 1 to an assigned word in a "data ready" vector, also residing in reflective memory. All DSPs spin-wait until this vector becomes all 1s. When this occurs, each DSP reads the error vector and clears its "data ready" location in reflective memory. Processing then proceeds. Each DSP will spin-wait on the 'ready' vector for a limited amount of time. If the time expires, the DSP signals an error to the control system and returns to waiting for the next feedback clock tic.

The master DSP continuously monitors slave performance. It monitors the "data ready" vector and identifies to the control system slaves that do not report "data ready" within time. Also, each slave DSP increments a heartbeat location in reflective memory that is monitored by the master. Slaves that fail to increment their heartbeat locations on each feedback clock tic are reported to the control system. Needless to say, these conditions indicate a malfunction and are dealt with by the APS operators.

Global controls, such as loop on/off, filter breakpoint frequencies, filter on/off, etc. are distributed to the slaves by the master via the reflective memory.

Software Development

The DSP software is developed on a Unix workstation using the Texas Instruments TMS3203x/C4x Code Generation tools. While most of the code is written in the C language, procedures that perform operations on arrays or vectors are written in C-callable assembly language routines. This allows us to insure that TMS320 DSP features such as parallel and three-operand instructions are used. The latest compiler (v 5.00) however seems to be much more sophisticated in optimization than prior versions. Nevertheless, we still prefer to use the assembly language routines.

Optimized code produced by the compiler can cause unexpected behavior, particularly when the compiler rearranges code to minimize DSP pipeline conflicts. This can be difficult to diagnose. We've uncovered "features" of the DSP VME interface that were stimulated by code rearrangement that improved speed.

Code is downloaded to the DSP via the controls LAN from the control system file server using tools in SwiftNet, a product available from the DSP vendor [5]. The tools run under VxWorks [6] on the VME controls processor located in the same crate as the DSP VME boards. The loader fetches executables via the LAN from a file server and transfers them over the VME bus to the DSP.

We have not made extensive use of vendor-supplied debugging tools, but have used reserved 'test' locations in dual-access RAM and in the reflective memories into which DPSs write selected values. These locations are easily interrogated from a

workstation via the VME controls processor. This method has little impact on the DSP algorithm and facilitates debugging at the normal sampling rate.

An important consideration in any real-time system is the time it takes for the code to operate. We've used two methods to measure this. The first method is to have each DSP write values to a VME DAC card, with a different value written after each major computation step. This allows the quick determination of where most time is consumed and is particularly useful with multiple DSP systems where each DSP accesses the VME bus, potentially causing bus contentions. Each DSP writes values to different DAC channels. System operation is easily observed on an oscilloscope connected to the DAC channels. The second timing method uses the DSP's on-chip timers to measure execution time. This method has minimal impact on execution, since no VME bus accesses are required, but does not easily lend itself to correlating execution of multiple processors.

Operational Issues

A great deal of effort has been spent in establishing reliable operation and in streamlining routine tasks to reduce the burden on the APS operators. For example, we ensure that no detectable transients are generated when the feedback loops are opened or closed. Transients are minimized by closing the loops with regulator settings that produce fast settling times, with the settings gradually ramped to their normal values.

On occasions it has been necessary to reconfigure the response matrix to remove misbehaving BPMs from the algorithm. Again, we have ensured that this can be performed with no impact on the users, other than having to open the control loops while the new matrix is downloaded via EPICS.

The system can also operate autonomously such that the control loops are automatically opened when stored beam is lost, and re-closed when the beam returns.

Efforts in these areas have paid off in terms of the overall reliability. During the first nine months that the orbit feedback system has been in routine operation with users, availability has been greater than 99%, and there has been only one beam dump directly attributed to it (leading to 42 minutes of machine downtime).

SYSTEM PERFORMANCE

On-line machine diagnostics make it possible to measure orbit motion quickly and conveniently. Typically, we measure the orbit motion at 40 BPMs located in the insertion-device straight sections, with power spectral density measurements averaged over the 40 locations.

We routinely measure the orbit motion over two frequency bands, one sampled at 60Hz (using the 'slow beam history' diagnostic [7]) and the other at orbit feedback system sampling rates. The slow beam history diagnostic is used to measure orbit motion in the frequency range 0.016Hz to 30Hz, while the real-time feedback system is used to measure orbit motion from 0.25Hz to 500Hz. Typical results of measurements during the latter part of the APS "98-2" user run are shown in Table 1.

TABLE 1. Typical Measured rms Orbit Motion at Insertion Device Source Points

	Horizontal		Vertical	
	Feedback Off	Feedback On	Feedback Off	Feedback On
Required orbit stability (rms) (with 10% x-y coupling)	17 μ m		4.5 μ m	
Orbit motion 0.016Hz-30Hz (rms)	18.4 μ m	4.4 μ m	3.1 μ m	1.8 μ m
Orbit motion 0.25Hz-500Hz (rms)	20 μ m	13.2 μ m	7.4 μ m	7.5 μ m
Typical beam size at source points (rms) ¹	335 μ m		18 μ m	
Beta at insertion device source points (design)	17m		3m	

¹Inferred from measurements at S35BM with 100mA beam, stored in 81 bunches.

It should be noted that even though the orbit feedback system is sampling at 1kHz, signal content up to 2kHz is included in the 0.25Hz-500Hz measurement because of aliasing of the incoming BPM data.

Horizontal and vertical power spectra in the band from 0.01Hz to 500Hz are shown in Figure 4. The same data are shown in Figure 5 as cumulative rms motion from 0.01Hz to 500Hz. This data was collected at three different sampling rates using the real-time orbit feedback system.

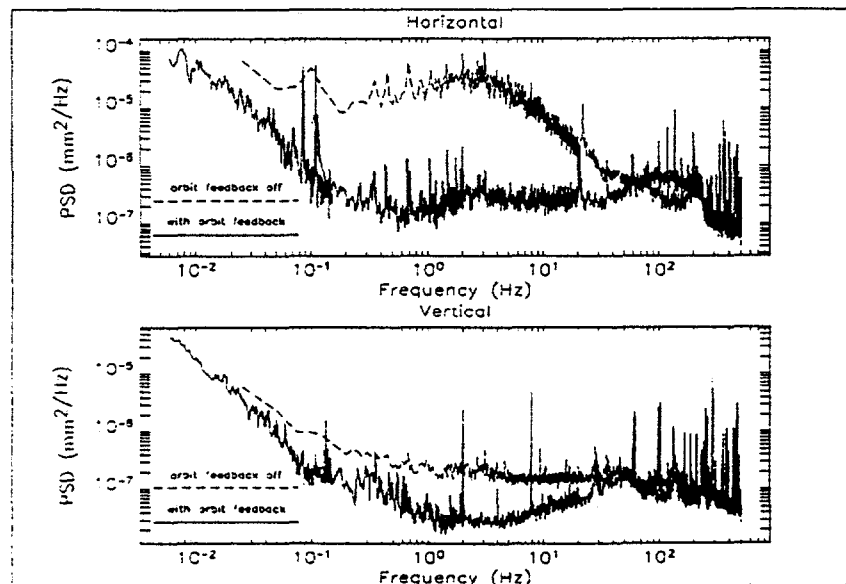


FIGURE 4. Orbit motion power spectra from 0.01Hz to 500Hz.

Horizontal orbit stability is well within the requirements in the band up to 500Hz. In the case of the vertical plane, orbit stability below 30Hz is within specification, but broad-band motion to 500Hz is still too high, although to date this has not been an issue with the APS users.

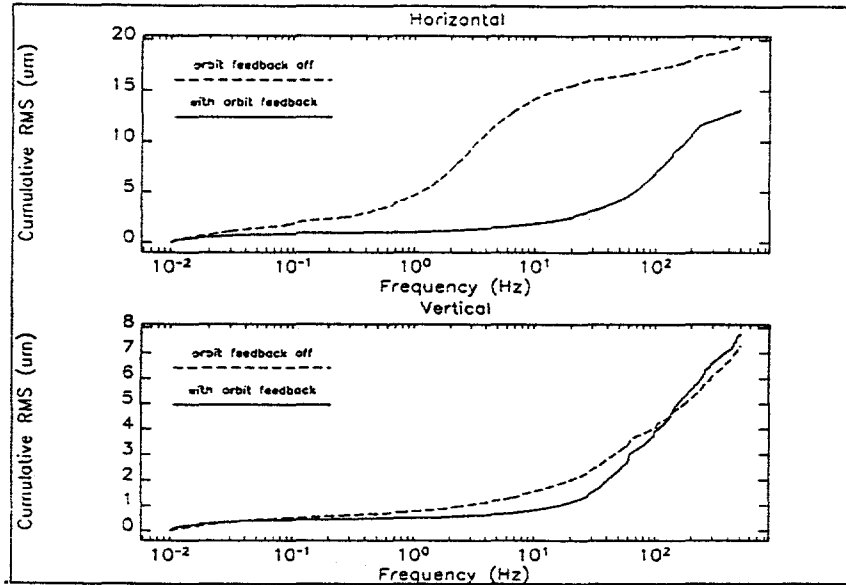


FIGURE 5. Cumulative rms orbit motion from 0.01Hz to 500Hz.

Horizontal orbit motion is dominated by power in the 0.1Hz to 20Hz frequency range. This is caused by small fluctuations in the current delivered to multipole magnets and corrector magnets in the storage ring (each magnet has a separate power supply). Fluctuations in the multipole magnet currents are converted into vertical AC dipole fields by the asymmetrical aluminum vacuum chamber. This effect is frequency dependent and peaks around 5Hz. The evidence for this is clearly visible in the horizontal power spectrum shown in Figure 4 (the peak is shifted to around 3Hz by the power spectrum of the power supply fluctuations). This contribution to orbit motion was unexpected, and was not taken into account when the power supply stability specifications were originally developed. Several narrow-band sources are visible in power spectra of both planes. These are caused by power converter ripple from the fast corrector power supplies that are not attenuated by the Inconel vacuum chamber. In most cases, their contribution to rms orbit motion is very small.

Two factors account for the fact that the orbit feedback system is more effective in reducing horizontal motion than vertical motion. First, the orbit feedback system is most effective in the frequency range that includes the horizontal motion between 0.1Hz and 10Hz. Conversely, since the vertical motion has a much flatter power spectrum, less of the power is included in the correction bandwidth. Second, the global algorithm itself is more effective in the horizontal plane, because more of the energy appears in spatial modes that are correctable by the feedback system. This has been

shown in modeling where the maximum theoretical attenuation in the horizontal plane was found to be around 22dB but only 15dB in the vertical plane.

An important factor in achieving optimum performance over a wide frequency range is the tuning of the feedback regulator. At present we use a simple bandpass filter and PID. By adjusting the PID settings it is possible to trade off a fast rise-time (i.e., wide correction bandwidth) against an overshoot in the step response (that results in amplification of higher frequencies). Depending on the power spectrum of the underlying motion, this trade-off can have a significant impact on the rms orbit motion. The effects of regulator tuning on measured rms orbit motion up to 30Hz and 500Hz are shown in Figure 6. Notice that while there is a clear optimum tuning for the horizontal plane, the broad-band vertical motion only increases when the regulator gain is increased. This is primarily because the vertical power spectrum is much flatter so that a reduction in low-frequency motion is achieved at the expense of higher-frequency motion.

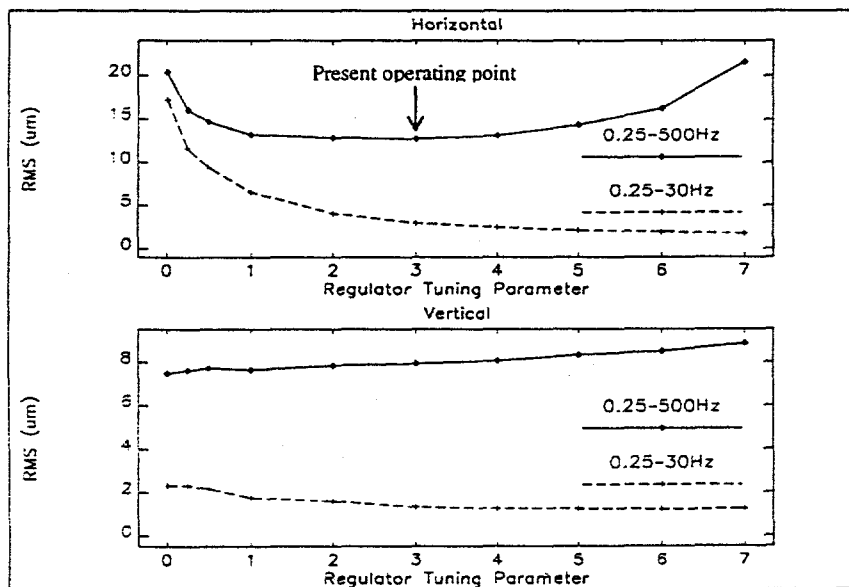


FIGURE 6. Measured rms orbit motion vs. regulator tuning.

Since the system does not currently allow different regulator settings for the two correction planes, the present regulator configuration was chosen as a compromise between the optimum setting for the two planes. As part of the upgrade to 2kHz, we will increase the order of the regulator filter and will include separate filters for each correction plane.

CORRECTOR EQUALIZATION

All of the 320 dual-function corrector magnets in the APS storage ring can be made available for real-time orbit feedback. However, the dynamics associated with the magnets vary depending on their location in the lattice because of eddy-current

effects in their associated vacuum chambers. Seven of the available eight corrector magnets in each sector are mounted on thick aluminum vacuum chambers, with the remaining corrector mounted on an Inconel bellows. Eddy-current effects in the aluminum chamber significantly impact field penetration to the particle beam by introducing a strong frequency dependence that slows the effective response of the corrector magnet. Eddy-current effects from the Inconel bellow have negligible impact and the response is dominated by power supply dynamics. In order to obtain the widest correction bandwidth, the global orbit correction system uses the 38 'fast' correctors available in each plane of the machine.

Figure 7 shows the step responses that were measured from the response of the closed orbit to a step change in setpoints to several of the magnets.

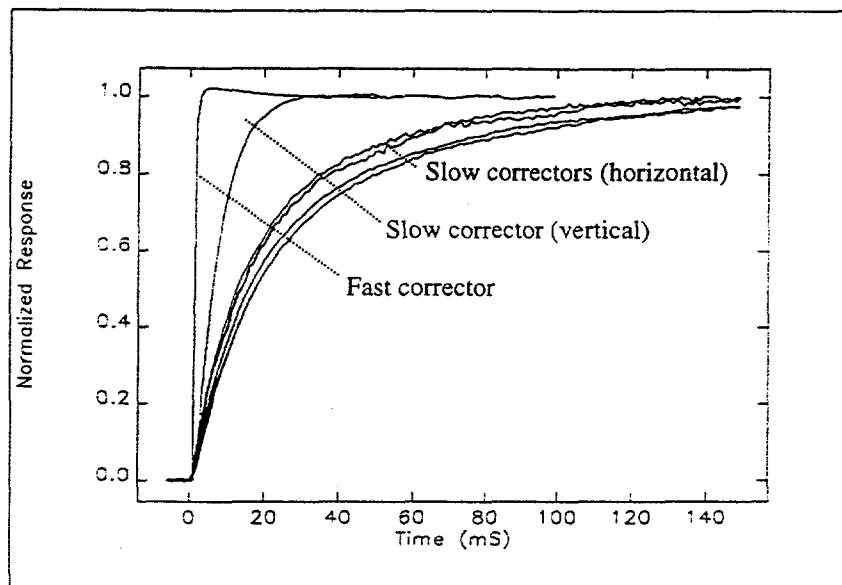


FIGURE 7. Dynamic orbit response to a step change in corrector setpoints.

Notice that there are significant differences between the step responses of horizontal and vertical windings for the 'slow' correctors. There are also slight differences in the responses of the four horizontal correctors that would be used to form a local bump around the insertion-device source point. The latter are caused by small differences in the vacuum chamber arrangements close to each of the magnets (e.g., there are pumping ports close to certain magnets). These differences in mechanical arrangements affect the eddy currents from stray fields of each magnet and result in subtle differences in the dynamics of each corrector. The differences are most problematic when correctors are combined to form local bumps that might be used to steer the particle orbit through the x-ray source points. Small differences in the step responses of the magnets are magnified by the large bump coefficients, and the resulting bumps become far from closed (i.e., they are non-local) dynamically.

It is possible to use the orbit feedback DSPs to implement equalization filters such that the combination of filter and magnet are identical in each case. One complication in designing the filters is that the eddy current effects are nonlinear with frequency and

cannot be exactly represented using a finite transfer function of poles and zeros. In modeling the responses of the correctors, we found that it is most effective to work in the time domain and to equalize measured step responses, rather than to equalize the frequency responses.

Even so, there are limitations to what can be achieved, particularly because of the time delay associated with the field penetration through the thick aluminum chambers. This means, for example, that it is not possible to equalize the slow correctors to give the same response as the fast correctors. So far, the most satisfactory results have been achieved by equalizing the correctors to a single-pole filter with a one-step time delay. Using a three-pole, three-zero discrete filter, it has been possible to equalize responses to within one part in a thousand. This is illustrated in Figure 8, where the equalized step response is shown together with original responses of the fast and slow correctors.

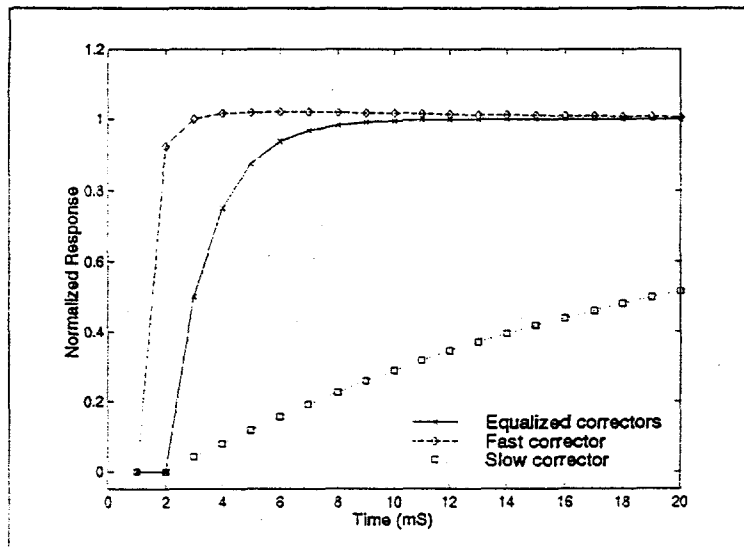


FIGURE 8. Equalized horizontal step response.

In all cases examined so far, the largest impulse applied to a corrector was a factor 20 higher than the desired step size. This is well within the dynamic range of the power supplies for any likely scenario.

While the equalized responses of the slow correctors are considerably faster than the original responses, there is some loss of bandwidth and increased phase delay with the fast correctors. If it is decided to implement a unified algorithm with both fast and slow (equalized) correctors, there will be a corresponding reduction in the maximum closed-loop bandwidth that can be achieved compared with a system that uses only fast correctors.

So far, the equalization filters have not been tested in the storage ring. It has been our experience that the optimization of the filter responses will be an iterative process because of contamination of the measured step responses by real orbit motion.

It should also be noted that the equalization filters have been designed for 1kHz orbit feedback operation. The transition to 2kHz should improve the overall result and may reduce the length of the time delay required in the equalized response.

ORBIT FEEDBACK AT X-RAY SOURCE POINTS

The APS real-time orbit feedback system was designed with both global and local feedback objectives in mind. However, implementation of the global feedback system was given priority over the local system since all users benefit from the improved global orbit stability. Indeed by using only global feedback, we have already met requirements for horizontal orbit stability. Nevertheless, local dynamic feedback will be implemented and will run in parallel with the existing global feedback algorithm.

Measurement of X-ray Beam Position

It has become clear that a usable local feedback system requires very stable high-resolution measurements of the x-ray source point or x-ray beam position. This has been most evident from experience with the workstation-based DC orbit correction system.

It was found that an algorithm that used many BPMs and relatively few correctors to correct the global rms orbit was more successful at stabilizing the x-ray source points than an algorithm that exactly corrected the rf BPMs around each source point. This is a consequence of current- and bunch pattern-dependence of the rf BPM offsets.

Photon BPMs are installed in each bending-magnet and insertion-device x-ray beamline and are specifically intended for use in local orbit feedback. By design, these offer much greater sensitivity and stability than the rf BPMs installed at the x-ray source points, and the photon BPMs installed in the bending magnet lines will shortly be integrated into the real-time feedback system. However, photon BPMs in the insertion-device beamlines are subject to x-ray contamination problems, not only from adjacent bending magnet x-ray sources, but also from quadrupole and corrector magnets that are in direct line-of-sight of the BPMs. To date, no simple method has been found to eliminate the measurement ambiguities from these sources, and accuracy of the insertion-device x-ray BPMs is limited to about $20\mu\text{m}$. Techniques are being developed for masking the stray radiation by physically moving accelerator components. These are scheduled for testing during the latter part of 1998.

In order to provide more stable DC measurements of the particle beam position, new (narrow-band) rf BPM electronics are being installed at each insertion device source point. These offer significant improvements over the present rf BPM electronics in terms of long-term drift and beam-current dependence, and it is anticipated that the combination of these narrow-band BPMs together with the photon BPMs will provide the stability required for local orbit feedback.

To manage the limited dynamic range of the photon BPMs, a virtual "mapped" BPM will be created that maps each photon BPM to an equivalent rf BPM location. In the event that the photon BPM signal becomes invalid, the rf BPM value will be automatically used in its place, alleviating the need to reconfigure the orbit correction response matrices.

Local Feedback Algorithms

The classic approach to local feedback is to create three- or four-corrector closed orbit bumps, where the ratios of corrector strengths are chosen to minimize global orbit effects from changing the local bump strength. There are practical difficulties with this approach since the bump coefficients must be very well matched (and possibly be frequency dependent) to eliminate closure errors. However, the algorithm is straightforward to implement since it requires only local BPM information.

A great advantage of the APS orbit feedback system is that every BPM in the storage ring is already available to the slave crates via reflective memory. This means that algorithms requiring access to global orbit information can be considered.

An important consideration in selecting a local algorithm is that the correctors available for local feedback have significantly slower responses than those of the global correctors because of eddy-current effects in their respective vacuum chambers. As was previously discussed, digital equalization of the corrector responses is certainly possible, but at some cost to the usable bandwidth of the global correctors.

The concept that is applied to the implementation of global feedback will also be applied to the local feedback system. All local orbit feedback loops will be incorporated into one (globally oriented) matrix. Additional corrector feedback loops will be implemented in the same way as the global system; each corrector control loop operates independently, with its feedback 'error' signal being derived from the vector dot product of one row of the new 'local' inverse response matrix and the vector of measured BPM errors. By changing the inverse response matrix contents and the regulator configuration, it will be possible to explore several different algorithms that are either unified with the existing global algorithm or operate independently.

Two algorithm structures are currently under consideration, one decoupled from the global matrix in the frequency domain and the other decoupled in the spatial domain. The first option uses local feedback to reduce dynamic motion at the x-ray source points up to a few hertz, while retaining the existing global feedback system to reduce higher frequency orbit motion. This solution probably offers the widest correction bandwidth because the global feedback corrector response would not have to be compromised by equalization.

The second option is to digitally equalize the frequency responses of all (slow and fast) correctors and to integrate both local and global objectives into a single response matrix. Suitable weighting of the x-ray source points in the inverse response matrix would provide exact correction at the source points themselves, with global rms orbit minimization everywhere else. While this would certainly offer the best correction in spatial terms, it would come at the expense of some global feedback bandwidth because of the need to equalize all the correctors to the same response.

In either structure, depending on the stability of the source point measurements, the correction bandwidth could continue down to DC, or be rolled off at some low frequency so as to mesh with the existing workstation-based global correction algorithm. The possibility of incorporating different correction bandwidths for global and local correction within the unified algorithm is also being explored.

REAL-TIME BEAM DIAGNOSTICS

The reflective memory provides the means to share data and distribute global controls. The use of reflective memory to share the BPM error vector has already been mentioned. In addition, each slave DSP deposits BPM positions, computed corrector values, and x-ray BPM data in reflective memory at the feedback clock rate. This data is accessible to the master DSP for collection and analysis.

To take advantage of this data, a number of diagnostics have been incorporated into the orbit feedback system. These include running statistics of quantities such as rms corrector 'errors' and capture of waveforms from any of the signals deposited into reflective memory by each slave station. Typical uses include tracking the rms orbit motion, measuring response matrices using an 'AC-lockin' technique, and post-analyzing orbit motion that resulted in a beam dump. The system has also proven to be very useful for identifying BPM and corrector channels that are misbehaving.

'Dspscope'

Any of the signals deposited into reflective memory can be accessed at the feedback sampling rate and collected as a waveform. A total of 40 waveforms can be collected simultaneously, each with up to 4080 data points. Lower data collection rates are achieved by filtering and decimating the incoming data. This tool is used to routinely collect BPM and corrector 'error' signals for orbit motion measurements.

'AC Voltmeter'

Any of the signals can also be Fourier analyzed in real time with a sliding discrete Fourier transform, so that the time evolution of particular frequency components can be followed. This has been most useful for 'AC-lockin' measurements, where the orbit feedback system drives a chosen corrector at one frequency (typically 83.33Hz) and measures the response at that frequency using the 'AC Voltmeter'. This technique has been successful in making rapid measurements of the response matrix and in identifying BPM gain errors.

Corrector 'Error' History Buffers

A corrector 'error' is defined as the result of the vector dot product of the measured positional errors (BPM 'errors') and the appropriate row of the inverse response matrix. As described in a later section, this signal is useful for localizing sources of orbit motion. The past 128 samples of corrector errors are stored in sliding buffers. When an unexpected beam dump occurs, the buffers are frozen and their contents automatically downloaded and archived with other information that can be used to trace the cause of the beam dump. These history buffers have proven useful in identifying the character of certain classes of beam dump and in localizing the origin of motion associated with it (a glitch on a magnet power supply, for example).

Sliding Algorithms

The 'AC Voltmeter' is one of several algorithms that have been implemented as 'sliding' algorithms, where previously-computed results are updated on every tick, as new data becomes available. In addition to the sliding Fourier transform, we have implemented statistical algorithms that estimate, for example, the mean and variance of the corrector error signals. The results are collected at periodic intervals and archived along with other machine data for subsequent analysis.

IDENTIFYING SOURCES OF ORBIT MOTION

The global orbit feedback algorithm uses 160 BPMs to determine corrections at 38 correctors in each plane. Since the forward response matrix is over-determined, the inverse response matrix is a least-squares solution that minimizes the rms of all BPM errors. The form of the matrix is band diagonal, meaning that each BPM influences only a subset of the correctors and that the response of each corrector is dominated by a subset of the BPMs. A practical implication is that for any given disturbance, orbit corrections are applied to magnets that are close to the source of the disturbance.

This feature has proved very useful in using orbit correction signals to localize strong sources of orbit motion. The 'dspscope' diagnostic in the orbit feedback system allows simultaneous data collection from all corrector drive signals or corrector 'error' signals in each plane at the full orbit feedback sampling rate. Taking the power spectral density of these signals, it is possible to generate a 'roadmap' of the sources of underlying orbit motion in the storage ring. An example is shown in Figure 9.

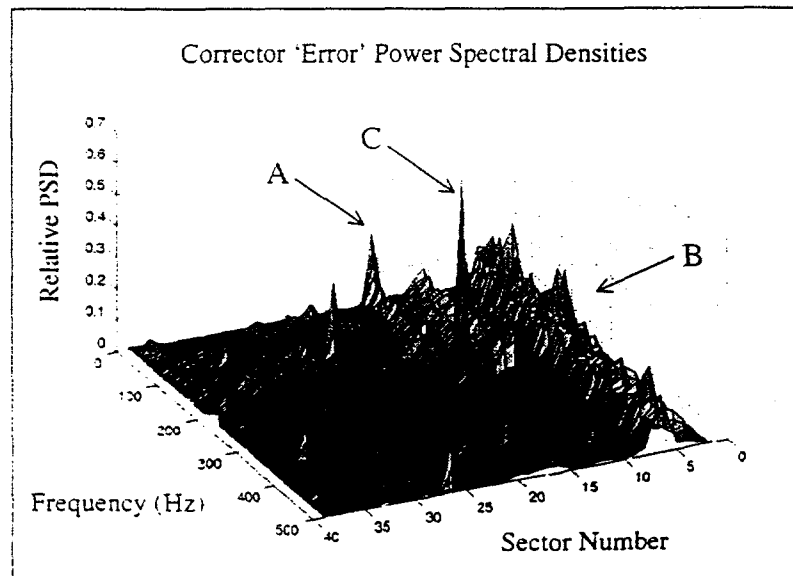


FIGURE 9. Example 'roadmap' of sources of horizontal orbit motion (see text for explanation of labeled features).

Three features are highlighted on the figure. Low-frequency broad-band orbit motion in sector 16 ('A') was identified as a sextupole power supply with poor regulation. Narrow-band motion at 250Hz, also in sector 16 ('B'), was identified as an oscillating corrector power supply. The wide-band orbit motion covering several sectors around sector 6 ('C') was identified as a bad BPM, and the indicated motion was not real. The bad BPM actually caused the orbit feedback system to generate motion, since the noisy BPM signal was interpreted as real beam motion. The spatial resolution of this technique for identifying sources of motion is actually better than the spacing between correctors. By examining patterns of adjoining correctors, it is possible to localize the source to about one third of a sector.

The number of corrector 'error' signals that are affected by a given source depends on the location of the source relative to adjacent feedback correctors. Patterns were measured by driving each of the ten quadrupoles in one sector with AC signals of equal magnitude and examining the response of the orbit feedback system. (Note that the AC modulation on the quadrupoles was converted to a vertical dipole field by the asymmetrical vacuum chamber.) Three separate patterns were identified and are shown in Figure 10. (More than three patterns can be identified if subtle differences are taken into account, although they have not proven to be useful in locating real sources of motion.)

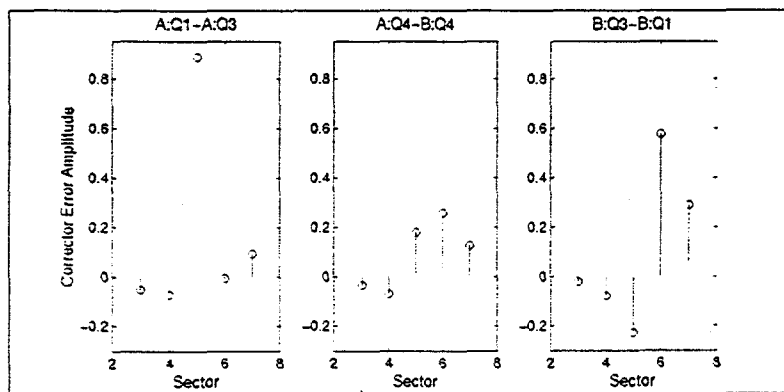


FIGURE 10. Horizontal corrector 'error' patterns for excitation of the ten different quadrupoles located in Sector 6.

The different corrector error patterns are associated with the location of the source within the sector in terms of betatron phase. The fact that we identified three separate patterns of correctors is consistent with there being two distinct changes in betatron phase advance through the lattice.

These beam-based techniques have proven useful in identifying a number of magnet power supplies with poor regulation and with small oscillations on their outputs. However, in certain cases, strong sources have been localized but the sources themselves have not been identified. We have also found there is a more definitive indication of source locations when the measured response matrix is used instead of the modeled response matrix that is generally used for orbit feedback.

FUTURE PROSPECTS FOR ORBIT STABILITY AT THE APS

It was noted earlier that even with orbit feedback, the wideband vertical orbit motion is out of specification. This is accentuated by the fact that the APS is now to routinely deliver beam with 1% x-y coupling, a number that is likely to be further reduced in the future. If we are to maintain orbit stability within 5% of the beam size at such small x-y coupling levels, orbit motion will ultimately have to be reduced below $1\mu\text{m}$ rms. This presents a tremendous challenge, not the least of which is our ability to measure and correct such small orbit motion.

For such small orbit motion requirements, an important consideration will be the frequency spectrum of the residual motion. While most users observe low frequency orbit motion as fluctuations in x-ray intensity, higher frequency motion is observed as an increase in the effective x-ray beam size. Consequently, it is reasonable to consider spectral shaping of the residual motion rather than to reduce the broad-band rms motion below certain absolute levels. (This is already being done to some extent with the choice of regulator tuning in the vertical plane.)

BPM Resolution and Stability

The need for stable and accurate measurements of the beam position has already been discussed within the context of local orbit feedback. The prospects for reducing global orbit motion to submicron levels are very much dependent on the quality of the beam position information provided by the rf and photon BPMs [8].

Provided we are able to accurately measure the trajectory of the x-ray beams, implementation of the local feedback algorithms should reduce x-ray beam motion significantly below present levels. The alternative is to continue to improve the performance of the global orbit feedback system, based on the premise that a large number of (relatively) poor sensors can provide more accurate information about the global orbit than a small number of (relatively) accurate sensors.

Global Orbit Feedback Improvements

Regardless of whether the local feedback system can be implemented, we will continue to work on improving the performance of the global algorithms.

The present algorithm contains 160 BPMs and 38 correctors, and will shortly correct the orbit at a 2kHz rate (presently 1kHz). However, there are many more BPMs and correctors available to the system, and with fixed processing power it is possible to trade off sampling rate against the number of elements (BPMs and correctors) used in the global algorithm. In terms of algorithm performance, the trade-off is in terms of correction bandwidth, signal-to-noise ratio, and number of spatial modes corrected.

The signal-to-noise ratio varies as the square root of the number of BPMs used. The spatial resolution also improves as the number of BPMs is increased, but there are diminishing returns as further BPMs are added. Modeling indicates that using four BPMs per sector (160 BPMs in total) gives an rms improvement of around 90% of the improvement obtained with all 360 BPMs.

The greatest impact on vertical orbit motion is expected from increasing the number of correctors in the global algorithm from 38 to 77 (two correctors per sector instead of one). This is estimated to increase the maximum attenuation of vertical motion from 15dB to 27dB. While this would not increase the range of correction, it would further attenuate the orbit motion within the present correction bandwidth.

Increasing the correction bandwidth of the existing feedback system would also help reduce wideband rms orbit motion. Without increasing the sampling rate beyond 2kHz, it is expected that the most significant improvements in correction bandwidth can be achieved by increasing the order of (and optimizing) the feedback regulator.

It should be noted that the VME bus backplane is rapidly becoming a bottleneck, with 50% of the total computation time being associated with accessing the BPM data from reflective memory. At this point, it would only be possible to increase the sampling rate significantly above 2kHz by reducing the number of BPMs in the global algorithm.

Corrector Quantization

The present corrector magnet power supplies have 16-bit resolution and a maximum kick of $\pm 1\text{mrad}$ that generates a peak orbit deviation of $\pm 10\text{mm}$ at the x-ray source points. Statistically, quantization errors caused by the finite resolution can be considered a white noise source with values uniformly distributed between ± 0.5 least-significant bits. This has an rms value of 0.29 bits, with energy equally distributed over the entire frequency band from DC to half the sampling rate. On the assumption that the effective resolution is 15 bits, then rms orbit motion caused by quantization errors of the 38 global correctors is estimated to be around $1.1\mu\text{m}$.

In order to reduce these quantization errors, a program is underway at APS to increase the resolution of the corrector power supplies. An alternative would be to reduce the dynamic range of the power supplies, but this approach is less desirable since it also reduces flexibility in steering the DC orbit.

Reducing the Magnitude of the Underlying Orbit Motion

Clearly the most effective method of reducing the rms orbit motion is to remove the underlying sources of the motion. The program of identifying strong sources of orbit motion is continuing, and work is also underway to improve the stability of the magnet power supplies that are presently dominating the orbit motion power spectra.

CONCLUSIONS

The real-time orbit feedback system implemented at the APS successfully reduces horizontal orbit motion below the specification of 5% of beam size. Vertical orbit motion up to 30Hz is also within specification, although broad-band vertical motion is still out of specification. To date, however, this has not been an issue with the APS users.

Local feedback is presently not implemented. Several options are available for its implementation in combination with the existing global orbit feedback algorithms. Initial evaluations of these options on the APS storage ring are anticipated to occur during the latter part of 1998.

There are several diagnostic capabilities built into the orbit feedback system that provide the ability not only to measure orbit motion and track system performance, but also to localize the sources of orbit motion.

Long-term plans for the APS include reducing vertical rms orbit motion to sub-micron levels. This provides a tremendous challenge in our ability to measure and correct very small orbit motions. It is expected that with continuing improvements, the system will meet this challenge.

ACKNOWLEDGEMENTS

The authors wish to thank J. Galayda for his continued support and encouragement in the development of this system. We also wish to thank M. Borland, G. Decker, and L. Emery for their encouragement and assistance with orbit correction and physics issues; and C. Doose, A. Hillman, D. McGhee, R. Merl, and A. Pietryla for their assistance with technical issues.

REFERENCES

- [1] Winick, H., ed., "Synchrotron Radiation Sources - A Primer," pp. 344-364, World Scientific (1994).
- [2] Emery, L., Borland, M.D., "Advances in Orbit Drift Correction in the Advanced Photon Source Storage Ring," *Proceedings of the 1997 Particle Accelerator Conference*, Vancouver BC, Canada, May 1997 (to be published).
- [3] Carwardine, J.A., Lenkszus, F.R., "Architecture of the APS Real-Time Orbit Feedback System," *Proceedings of the 1997 International Conference on Accelerator and Large Experimental Physics Control Systems*, Beijing, China, November 1997 (to be published).
- [4] Lenkszus, F.R., Laird, R., "The Advanced Photon Source Event System," *Proceedings of the 1995 International Conference on Accelerator and Large Experimental Physics Control Systems*, Vol. 1, pp. 345-350 (1996).
- [5] Wind River Systems, Alameda, CA 94501.
- [6] Pentek, Upper Saddle River, NJ 07458.
- [7] Lenkszus, F.R., et al., "Beam Position Monitor Data Acquisition System for the Advanced Photon Source," *Proceedings of the 1993 Particle Accelerator Conference*, Washington DC, USA, May 1993, pp. 1814-1816 (1993).
- [8] Decker, G.D., Carwardine, J.A., Singh, O.V., "Fundamental Limits on Beam Stability at the Advanced Photon Source," these proceedings.